# A Multi-Objective Approach to Indoor Wireless Heterogeneous Networks Planning Based on Biogeography-Based Optimization

Sotirios K. Goudos[*a], David Plets[b], Ning Liu[b], Luc Martens[b], Wout Joseph[b]

[a]Radiocommunications Laboratory, Department of Physics, Aristotle University of Thessaloniki, GR-54124 Thessaloniki, Greece

[b]WiCa, Ghent University / iMinds, Dept. of Information Technology, Gaston Crommenlaan~8~box~201, B-9050 Ghent, Belgium

*Corresponding author: Tel :+302310998392 Fax:+302310998069 email :sgoudo@physics.auth.gr

Radiocommunications Laboratory, Department of Physics, Aristotle University of Thessaloniki,

GR-541 24 Thessaloniki, Greece

**Abstract—In this paper, we present a multi-objective optimization approach for indoor wireless network planning subject to constraints for exposure minimization, coverage maximization and power consumption minimization. We consider heterogeneous networks consisting of WiFi Access Points (APs) and Long Term Evolution (LTE) femtocells. We propose a design framework based on Multi-objective Biogeography-based Optimization (MOBBO). We apply the MOBBO algorithm to network planning design cases in a real office environment. To validate this approach we compare results with other multi-objective algorithms like the Nondominated Sorting Genetic Algorithm-II (NSGA-II) and the Generalized Differential Evolution (GDE3) algorithm. The results of the proposed method indicate the advantages and applicability of the multi-objective approach.**

**Keywords— Indoor wireless network planning, heterogeneous networks, exposure minimization, biogeography-based optimization, differential evolution, genetic algorithms, generalized differential evolution, Pareto optimization, multi-objective Optimization.**

## 1. Introduction

Wireless network design problems are in general multi-objective. Common design objectives include exposure minimization, coverage maximization, power consumption minimization and cost reduction [1-6]. Due to the increased popularity of indoor wireless networks, many software tools have been developed for the prediction of the received signal quality and the network performance [7-11]. These tools are based on either ray models, numerical solver models, heuristic predictions, or statistical (site-specific) models. In [12], the authors developed a heuristic indoor propagation prediction tool, which is able to design and optimize a WiFi network for a given coverage requirement with a minimal number of access points (APs). In the meanwhile, both the trend towards green networking [13, 14] as well as the enormous increase of wireless communication due to the increasing need for coverage and high data rates, make it necessary to investigate and characterize the exposure of the general public to electromagnetic fields at RF (radio-

frequency) frequencies used for wireless communications. Measurements and studies have indicated that indoor exposure cannot be neglected [15]. International safety guidelines such as [16] and those from ICNIRP (International Commission on Non-Ionizing Radiation Protection) [17] have been developed and authorities and countries have implemented laws and norms to limit human exposure. This indicates the need for an accurate exposure characterization and exposure-aware network planning. Additionally, research has recently been started on green network deployments [13, 18] in order to limit energy consumption in wireless (access) networks.

The Evolutionary Algorithms (EAs) mimic behaviour of biological entities and they are inspired from Darwinian evolution in nature. The EAs have been extensively studied and applied to several real-world engineering problems. Among others, EAs include genetic algorithms (GA), particle swarm optimization (PSO) [19], and differential evolution (DE) [20]. Generalized Differential Evolution (GDE3) [21] is a multi-objective DE algorithm that has outperformed other multi-objective evolutionary algorithms for a given set of numerical problems [22, 23]. GDE3 has been applied to microwave filter design in [24], Yagi antenna design in [25], and subarray design in [26]. Nondominated Sorting Genetic Algorithm-II (NSGA-II) [27] is a popular and efficient multi-objective genetic algorithm for solving real world engineering problems [28, 29].

Biogeography-based optimization (BBO) [30] is a recently introduced evolutionary algorithm. BBO is based on mathematical models that describe how species migrate from one island to another, how new species arise, and how species become extinct. The way the problem solution is found is analogous to nature's way of distributing species. In the BBO approach there is a way of sharing information between solutions [30], similar to the other evolutionary algorithms such as GAs, DE, and PSO. This feature makes BBO suitable for the same types of problems that the other algorithms are used for, namely high-dimensional data. Additionally, BBO has some unique features, which are different from those found in the other evolutionary algorithms. For example, quite different from GAs, DE and PSO, the set of the BBO's solutions is maintained from one generation to the next and is improved using the migration model, where

the emigration and immigration rates are determined by the fitness of each solution. These differences can make BBO outperform other algorithms [30]. BBO has been applied successfully to several real world engineering problems [31-39].

In this paper, we use a multi-objective extension of the BBO algorithm (MOBBO) combined with the concept of non-dominated ranking found in NSGA-II and GDE3. Amongst others, multi-objective BBO is applied in [40] for optimal PMU placement, in [41] for feature selection using gene expression data, and in [42] for robot path planning.

Therefore, we apply both the above-mentioned multi-objective evolutionary algorithms to the heterogeneous wireless network planning problem. With heterogeneous, we mean a combination of different wireless technologies, namely WiFi APs and Long-Term Evolution (LTE) femtocells. We define this problem as one with three objective functions. We consider an objective function for exposure minimization, coverage maximization, and power consumption minimization. To the best of the authors' knowledge, this is the first time that the BBO algorithm is applied to the specific design problem. The novelty in our work lies also in the fact that we propose a multi-objective framework by defining specific objective and constraint functions and using multi-objective evolutionary algorithms for solving such problems. The advantages of our approach are clearly shown for the first time for multi-objective network planning problems.

This paper is organized as follows. We describe the problem formulation in Section 2. The details of the BBO and the MOBBO algorithms are given in Section 3. In Section 4 we present the numerical results. Finally, the conclusion is given in Section 5.

## 2. Problem formulation

### *2.1 Configuration*

We consider the ground plan of an office building in Ghent, Belgium to which the network planning optimization will be applied (Fig. 1). It is a 90 m (length) by 17 m (width) office environment. The grey

walls are concrete walls, the brown walls are layered drywalls. Concrete walls have higher penetration loss and attenuate the signal more. The red dots indicate rooms where no wireless coverage is required, since they are (e.g., elevators, sheds, kitchens). For the considered model (IEEE TGn model), the walls will have no impact, as this model implicitly accounts for 'a typical wall presence in an office environment' with a well-chosen path-loss intercept and slope.

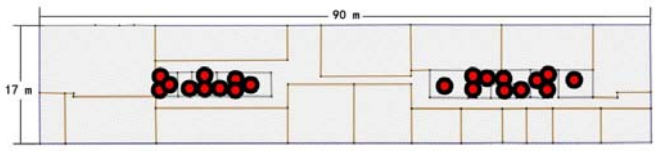


Fig. 1 Map of the ground plan

WiFi (IEEE 802.11n) access points at 2.4 GHz will be installed at a subset of $N_L$ possible locations in the building. We consider $N_L$ to be 425. The assumed receiver antenna gain is 0 dBi and a received power of −68 dBm is required to obtain a capacity of 54 Mbps. There are also 425 receiver location for which coverage and exposure level will be calculated. For reasons of implementation ease, the total pool of possible AP locations is chosen at the locations as determined by the receiver locations grid**.** The PL will be modeled according to two-slope model proposed by the IEEE 802.11 TGn channel models group [43]:

$$PL(d) = \begin{cases} PL_{freespace}(d) + \mathrm{X}(d \le 10m) \\ PL_{freespace}(d) + 32\log_{10}(\frac{d}{10}) + \mathrm{X}(d > 10m) \end{cases} \quad (1)$$

with $PL_{freespace}(d)$ the free-space path loss, and d the distance (m) between transmitter and receiver. X is the lognormal variation of the path loss around the model and has a standard deviation equal to 3 dB for d ≤10m and 5 dB for d> 10m. This corresponds to 95%-shadowing margins of 4.92 dB (d ≤10m) and 8.20 dB (d >10m). The 99%-temporal fading margin is set at 5 dB [44].

The path loss model for LTE only (slightly) differs from the WiFi PL model in the free-space loss part of eq. (1) in [12], due to the frequency dependence. Wall penetration losses and interaction losses (see eq. (1) in [12]) are assumed the same, since the LTE and WiFi frequencies are very similar (2.6 GHz vs. 2.4 GHz). Although several frequency bands have been assigned to LTE operation, in this paper we consider the 2.6

GHz frequency band. Additionally, we must point out that interfemto interference is not being considered in this paper.

For construction of the exposure model, we use the far-field conversion formula between path loss and electric-field strength defined in [45]:

$$PL[dB] = 139.3 - E_{ERP=1kW}[dB\mu V/m] + 20\log_{10} f[MHz] \quad (2)$$

where $PL[dB]$ is the path loss between the transmitter and a receiver at a certain location, $E_{ERP=1kW}[dB\mu V/m]$ is the received field strength for an Effective Radiated Power (ERP) of 1 kW, and $f[MHz]$ is the frequency.

Using Equation (2) and the identity

$$E[V/m] = E_{ERP=1kW}[dB\mu V/m] \times \sqrt{ERP[kW]} \quad (3)$$

and knowing that for dipoles $ERP[dBm] = EIRP[dBm] - 2.15$, we obtain the following formula for the electric field strength $E[V/m]$ at a certain location, as a function of the Equivalent Isotropically Radiated Power (EIRP) , the path loss, and the frequency:

$$E[V/m] = 10^{\frac{EIRP[dBm] - 43.15 + 20\log_{10} f[MHz] - PL[dB]}{20}} \quad (4)$$

*2.2 Mathematical formulation*

The network-planning problem is to find the AP characteristics (position and EIRP) in such a way that the power consumption is minimized, the human exposure to electric fields is minimized, and the coverage is maximized. All the above objectives are subject to constraints regarding coverage and exposure limits. Furthermore, since we consider a heterogeneous network, at least one LTE femtocell should be present. The coverage requirement depends on the capacity in Mbps and therefore on the receiver sensitivity that is required in each case. We consider that a point is covered according to received power level, if that is above or equal to the dBm limit for that case then the point is considered covered. The receiver

sensitivities of the WiFi and LTE receivers for a 20MHz channel are shown in Table 1 of [46]. It should be noted that the provided capacity is calculated from an AP point-of-view. When multiple users are connected to a certain base station or AP, the throughput per user might decrease. Additionally, we assume that we minimize power consumption by minimizing the number of turned on APs. It was shown in [18] that the RF power is responsible for only a small fraction of the total consumed power. The power consumption is determined by the number of APs, since the RF transmit power only has a minimal influence on the total power consumption: the RF power is small (at most 0.1W) compared to the power consumption of the other hardware in the AP (around 12 W). With respect to power consumption, it is therefore advisory to deploy APs at their maximum transmit power, which will correspond to a network with a minimal number of APs. However, a drawback of such high transmit power, is an increased human exposure. Therefore, the total power can be assumed to be equal to 12W, while the RF power is (for WiFi) limited to 20dBm or 100mW. This is valid for both WiFi APs and LTE femtocell base stations (For an LTE femtocell, there will be a slight additional difference due to the power amplifier efficiency, but this difference is very limited and can be neglected ).

Such a problem is inherently multi-objective. It can be defined by the minimization of the objective functions given below:

$$f_1(\overline{x}) = N_{AP}^{on} \quad \text{minimize power consumption} \tag{5}$$

$$f_2(\overline{x}) = -100 \times \frac{C_{sol}(\overline{x})}{C_{tot}(\overline{x})} \quad \text{maximize coverage} \tag{6}$$

$$f_3(\overline{x}) = E_{median}(\overline{x}) \quad \text{minimize exposure} \tag{7}$$

subject to:

$$g_1(\overline{x}) = \left| f_2(\overline{x}) \right| \geq C_{limit} \quad \text{coverage limit} \tag{8}$$

$$g_2(\overline{x}) = f_3(\overline{x}) \leq E_{limit} \quad \text{exposure limit} \tag{9}$$

$g_3(\overline{x}) = N_{LTE}^{on} \geq 1$ at least one LTE femtocell is present,

where $\overline{x}$ is the vector of decision variables, $N_{AP}^{on}$ is the total number of base stations (both LTE and WiFi)

that is turned on, $N_{LTE}^{on}$ the number of turned on LTE femtocells, $C_{limit}$ the coverage percentage required (0-100), $E_{limit}$ the desired electric-field maximum median value (V/m), $E_{median}$ the calculated electric field median value (V/m), $C_{sol}$ is the number of reception points covered by the current solution in this indoor environment, and $C_{tot}$ is the total number of all reception points in the building floor.

The decision variables are the first $N_L$ variables that represent the AP type and the next $N_L$ variables that represent possible EIRP values. The first $N_L$ variables could have a value of 0 (no AP turned on), 1 (WiFi AP turned on), or 2 (LTE femtocell turned on). The range of the possible EIRP values is from 0 to 20 dBm (100 mW) for both the WiFi and the LTE APs. Fig. 2 shows an example of unknown variables vector.

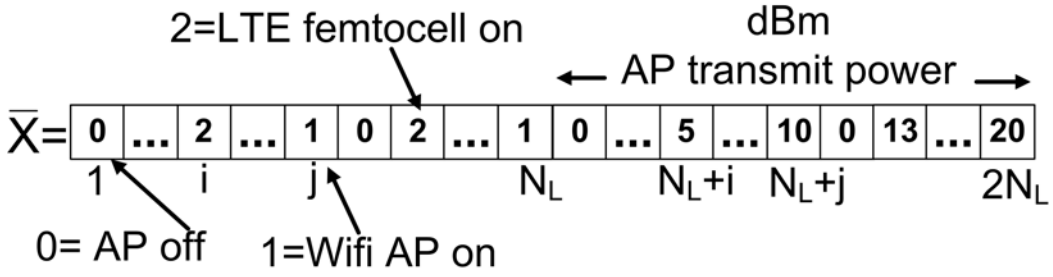


Fig.2 Structure of an example vector

The above-mentioned problem can be solved using a multi-objective evolutionary algorithm. It is a NP-hard integer-programming problem, for which several different solutions exist. The main goal is to find some points (solutions) that belong to the Pareto front. From this set of non-dominated solutions, optimal network configurations that provide a suitable compromise between the objectives for the desired constraints can be realized. We therefore apply the MOBBO the above-mentioned problem. In order to evaluate its performance, MOBBO is compared with NSGA-II and GDE3.

# 3. Algorithm Description

## *3.1 Biogeography-based optimization (BBO)*

The mathematical models of Biogeography are based on the work of Robert MacArthur and Edward Wilson in the early 1960s. Using this model, they have been able to predict the number of species in a habitat. The habitat is an area that is geographically isolated from other habitats. The geographical areas that are well suited as residences for biological species are said to have a high habitat suitability index (HSI). Therefore, every habitat is characterized by the HSI which depends on factors like rainfall, diversity of vegetation, diversity of topographic features, land area, and temperature. Each of the features that characterize habitability is known as suitability index variables (SIV). The SIVs are the independent variables while HSI is the dependent variable.

Therefore, a solution to a D-dimensional problem can be represented as a vector of *SIV* variables $\left[SIV_1, SIV_2, .....SIV_D\right]$, which is a habitat or island. The value of HSI of a habitat is the value of the objective function that corresponds to that solution and it is found by

$$HSI = F\left(habitat\right) = F\left(SIV_1, SIV_2, .....SIV_D\right) \tag{10}$$

Habitats with a high HSI are good solutions of the objective function, while poor solutions are those habitats with a low HSI. The habitats with high HSI are those that have large population and high emigration rate $\mu$. For these habitats, the immigration rate $\lambda$ is low. The immigration and emigration rates are functions of the rank of the given candidate solution. The rank of the given candidate solution represents the number of species in a habitat. These are given by

$$\mu_k = E\left(\frac{k}{S_{\max}}\right), \quad \lambda_k = I\left(1 - \frac{k}{S_{\max}}\right) \tag{11}$$

here $I$ is the maximum possible immigration rate, $E$ is the maximum possible emigration rate, $k$ is the

rank of the given candidate solution, and $S_{\max}$ is the maximum number of species (e.g. population size). The rank of the given candidate solution or the number of species is obtained by sorting the solutions from most fit to least fit, according to the HSI value (e.g. fitness). That is the best candidate solution has a rank of $S_{\max}$ and the worst candidate solution has a rank of one. BBO uses both mutation and migration operators. The application of these operators to each SIV in each solution is decided probabilistically. In each generation, there is a probability $P_{\text{mod}} \in [0, 1]$ that each candidate solution will be modified by migration. $P_{\text{mod}}$ is a user-defined parameter that is typically set to a value close to one, and is analogous to crossover probability in GAs. That is the migration operator in each generation is applied only if $P_{\text{mod}}$ is greater than a random number generated from a uniform distribution from the interval [0,1).

The migration for *NP* habitats can be described as follows:

**Algorithm 1** Habitat migration

1: **for** *i*=1 to *NP*
2: Select $X_i$ with probability based on $\lambda_i$
3: **if** $rnd(0,1) < \lambda_i$ **then**
4: **for** *j*=1 to *NP*
5: Select $X_j$ with probability based on $\mu_j$
6: **if** $rnd(0,1) < \mu_j$ **then**
7: Randomly select a *SIV* $\sigma$ from $X_j$
8: Replace a random *SIV* in $X_i$ with $\sigma$
9: **end if**
10: **end for**
11: **end if**
12: **end for**

The $X_i$ in the above algorithm is habitat *i*. The information sharing between habitats is accomplished using the immigration and emigration rate. The $\lambda_i$ is proportional to the probability that SIVs from neighboring habitats will migrate into habitat $X_i$. The $\mu_i$ is proportional to the probability that SIVs from habitat $X_i$ will migrate into neighboring habitats.

The mutation rate *m* of a solution *S* is defined to be inversely proportional to the solution probability and it is given by

$$m_S = m_{\max}\left(\frac{1-P_s}{P_{\max}}\right) \tag{12}$$

where $P_s$ is the probability that a habitat contains *S* species (e.g. the rank of the solution is *S*), $P_{\max}$ is the maximum $P_s$ value over all $s \in [1, S_{max}]$, and $m_{\max}$ is a user-defined parameter. Simon in [30] described how $P_s$ changes from time *t* to time $t+\Delta t$ as

$$P_s(t+\Delta t) = P_s(t)\left(1-\lambda_s\Delta t-\mu_s\Delta t\right)+P_{s-1}(t)\lambda_{s-1}\Delta t+P_{s+1}(t)\mu_{s+1}\Delta t \tag{13}$$

According to [30] the above equation holds because in order to have s species at time $t+\Delta t$, one of the following conditions must hold:

a) There were *s* species at time *t* and no immigration or emigration occurred between *t* and $t+\Delta t$; or b) there were *s-1* species at time *t*, and one species immigrated; or c) there were *s+1* species at time *t*, and one species emigrated. Assuming that $\Delta t$ is small enough, the probability of more than one immigration or emigration can be ignored. Therefore, by setting $\Delta t \to 0$ the species count probability equation becomes

$$\dot{P}_s = \begin{cases} -\left(\lambda_s+\mu_s\right)P_s+\mu_{s+1}P_{s+1}+\lambda_{s-1}P_{s-1} & S < S_{\max} \\ -\left(\lambda_s+\mu_s\right)P_s+\lambda_{s-1}P_{s-1} & S = S_{\max} \end{cases} \tag{14}$$

where $\dot{P}_s$ is the species count probability matrix.

Mutation can be described as follows:

**Algorithm 2** Habitat mutation

```
1: for i=1 to NP
2:     Compute the probability P_i
3:     Select SIV X_i(j) with probability based on P_i
4:     if rnd(0,1) < m_i then
5:         Replace X_i(j) with a randomly generated SIV
6:     end if
7: end for
```

The $m_i$ in the above algorithm is the mutation rate of solution *i*.

As with other evolutionary algorithms, BBO also incorporates elitism. This is implemented with a user-selected elitism parameter *p*. This means that the *p* best solutions remain from one generation to the other. More details about the BBO algorithm can be found in [30].

### *3.2 Multi-objective Biogeography-based Optimization (MOBBO)*

The general constrained multi-objective optimization problem (MOOP) definition is [47]:

Minimize $\overline{f}(\overline{x}) = [f_1(\overline{x}), f_2(\overline{x}), .., f_n(\overline{x})]$ (15)

Subject to $g_i(\overline{x}) \le 0 \; i = 1, 2, .., k$ (16)

$\overline{f}(\overline{x})$ is the vector of the objective functions, $\overline{x}$ is the vector of design or decision variables, $f_i$, $g_i$ are the objective and the constraint functions respectively, $n$ is the number of objective functions and $k$ is the number of constraint functions. If $X$ is the search space and $Z$ is the objective space, then the vector of the objective functions $\overline{f}: X \to Z$ assigns to each vector $\overline{x} \in X$ a corresponding objective vector

$\overline{z} = \overline{f}(\overline{x}) \in Z$ . An *ideal point* (also called *utopia point*) $\overline{z}^*$ is called a vector of the objective space composed of the best objective function values:

$$z_j^* = \min\left\{ z_j \mid \overline{z} \in Z \right\} \quad j = 1,..,n \tag{17}$$

In principle, multi-objective optimization is different from single-objective optimization. In single-objective optimization, one attempts to obtain the best solution, which is usually the global minimum or the global maximum depending on the optimization problem. In case of multiple objectives, there may not be only one solution, which is the best (global minimum or maximum) with respect to all objectives. Pareto-optimal solutions are those solutions (from the set of feasible solutions) that cannot be improved in any objective without causing degradation in at least one other objective. If an obtained solution is improved so that at least one objective improves and the other objectives do not decline, then the newly found solution dominates the original solution. The goal of Pareto-optimization is to find the set of solutions that are not dominated by any other solution, which are called non-dominated solutions. The set of these solutions is called the Pareto Front.

EAs use vectors to model the possible solutions. In order to distinguish the members of the non-dominated set from the population members we refer to the first ones as solutions and to the second ones as vectors. The definitions of dominance relations between two vectors (or individuals of the population) are provided below. The weak dominance $\preceq$ relation between two vectors $\overline{x}_1, \overline{x}_2$ in the search space is defined as [21]:

- $\overline{x}_1$ weakly dominates $\overline{x}_2$
  $\overline{x}_1 \preceq \overline{x}_2$ iff $\forall i : F_i(\overline{x}_1) \le F_i(\overline{x}_2)$ (18)

  while the dominance $\prec$ relation is defined as:

- $\overline{x}_1$ dominates $\overline{x}_2$
  $\overline{x}_1 \prec \overline{x}_2$ iff $\overline{x}_1 \preceq \overline{x}_2 \wedge \exists i : F_i(\overline{x}_1) < F_i(\overline{x}_2)$ (19)

  The above relations can be extended to include constraint dominance $\prec_c$ [21]:

- $\overline{x}_1$ constraint-dominates $\overline{x}_2$, $\overline{x}_1 \prec_c \overline{x}_2$

when any of the following conditions are true:

1) $\overline{x}_1$ belongs to the feasible design space and $\overline{x}_2$ is infeasible.

2) $\overline{x}_1, \overline{x}_2$ are both infeasible but $\overline{x}_1$ dominates $\overline{x}_2$ in constraint function space.

3) $\overline{x}_1, \overline{x}_2$ both belong the feasible design space but $\overline{x}_1$ dominates $\overline{x}_2$ in objective function space.

Multi-objective BBO algorithms extend the original BBO algorithm for solving MOOP. The results found by an evolutionary algorithm are also called Pareto set approximation or approximation set. MOBBO is the hybridization between BBO and uses concepts common in other MO algorithms like NSGA-II and GDE3. To the best of the authors' knowledge this is the first time that a multi-objective algorithm is applied to the network design problem. The MOBBO flowchart is given in Fig. 3.

The MOBBO algorithm is outlined below:

1) Initialize the BBO control parameters. Map the problem solutions to SIVs and habitats. Set the habitat modification probability $P_{\text{mod}}$, the maximum immigration rate $I$, the maximum emigration rate $E$, the maximum migration rate $m_{\max}$ and the elitism parameter $p$ (if elitism is desired).

2) Initialize a random population of $NP$ habitats (solutions) from a uniform distribution. Set the number of generations $G$ to one.

3) Evaluate objective function and constraint function values.

4) Apply non-dominated ranking to $NP$ habitats. Compute (HSI) for each habitat of the population based on non-dominated ranking. The non-dominated ranking refers to sorting of the vectors regarding non-domination. This sorting approach is called Fast Non-dominated Sorting Approach and is described in detail in [27]. A brief description of this approach follows. First, for each habitat (solution) $i$ two values are calculated: a) the domination count $n_i$, (i.e the number of solutions which dominate the solution $i$) , and b) $S_i$, a set of solutions that the solution $i$ dominates. This requires comparisons. All solutions in the first nondominated front will have their domination count as zero. Now, for each solution $i$ with $n_i = 0$, we visit each member (j) of its set and reduce its domination count by one. In doing so, if for any member $m$

the domination count becomes zero, we put this member in a separate list *M*. These members belong to the second nondominated front. Now, the above procedure is continued with each member of *M* and the third front is identified. This process continues until all fronts are identified. An important operator for sorting habitats (e.g. computing HSI value) is the Crowded-Comparison operator ($\prec_n$) defined in [27].We assume that every habitat *k* in the population has two attributes: a) nondomination rank ($k_{rank}$); and b) crowding distance ($k_{\text{distance}}$). The Crowded-Comparison operator is defined as:

$$k \prec_n q \ if \ \ k_{rank} < q_{rank} \ or \left(k_{rank} = q_{rank} \ \ and \ \ k_{\text{distance}} > q_{\text{distance}}\right)$$

Therefore, between two habitats with differing nondomination ranks, we prefer the habitat with the lower (better) rank. Otherwise, if both habitats have the same rank, we select the habitat that is located in a lesser crowded region.

5) Map the HSI value to the number of species *S.* That is sort the population from most fit to least fit and then assign a rank or number of species from 1 (best) to *NP(worst).* Calculate the immigration rate $\lambda_k$, the emigration rate $\mu_k$ for each solution of the population.

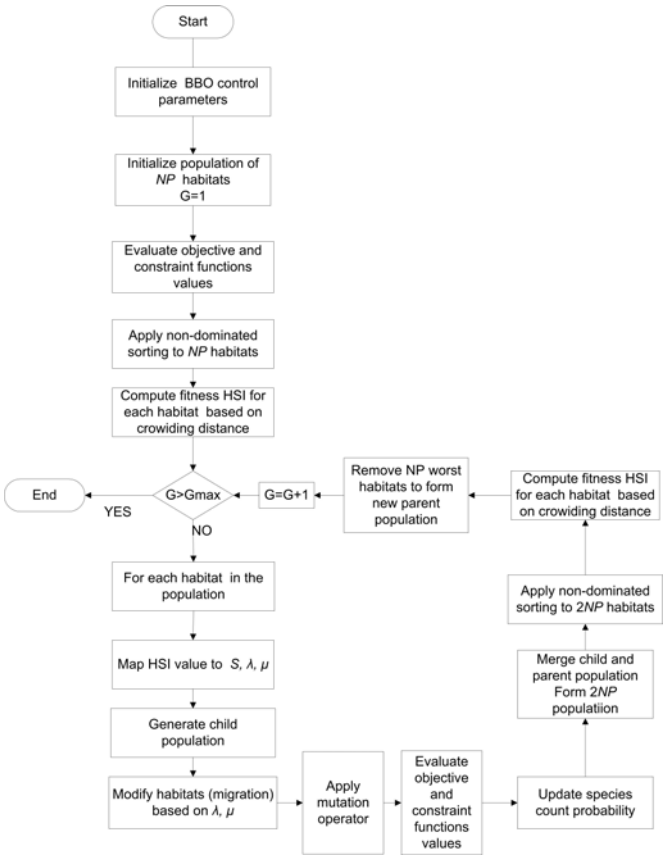


Fig. 3 MOBBO flowchart

6) Generate a new child population of $NP$ habitats, which is originally the same as the parent population.

7) Apply the migration operator for each member of the child population based on immigration and emigration rates using (11).

8) Update the species count probability according to (14).

9) Apply the mutation operator to each member of the child population according to (12).

10) Evaluate objective function and constraint function values. 11) Merge original parent population with new child population to form a population 2*NP* habitats.

12) Apply non-dominated ranking to 2*NP* habitats. That is according to the level of non-domination, each solution must be compared with every other solution in the population to find if it is dominated. Select the first $NP$ ranked habitats, which are the new parent population. That is we sort the solutions using the crowded-comparison operator in descending order and choose the best $NP$ solutions.

13) Repeat step 5 until the maximum number of generations $G_{\max}$ is reached.

To decrease the population back to the original size a sorting technique is applied. This uses the concept of Crowding Distance (CD), which approximates the crowdedness of a vector in its non-dominated set like NSGA-II [27]. The vectors are sorted based on non-dominance and crowdedness. The worst population members are removed and the population size is set to the original size. The basic idea is to prune a non-dominated set to have a desired number of solutions in such a way that the remaining solutions have as good diversity as possible, meaning that the spread of extreme solutions is as high as possible, and the relative distance between solutions is as equal as possible. The pruning method of NSGA-II provides good diversity in the case of two objectives, but when the number of objectives is more than two, the obtained diversity declines drastically [48]. MOBBO uses the same method used in GDE3, which is based on a crowding estimation technique using nearest neighbors of solutions in Euclidean sense, and a technique for finding these nearest neighbors quickly. More details about this pruning method can be found in [49]. Therefore, the selection based on Crowding Distance is improved over the original method of the NSGA-II to provide a better-distributed set of vectors.

## 4. Numerical Results.

We consider 425 different possible AP positions placed at a height 200 cm above ground level and the receiver is assumed at a height 100 cm above ground level (Fig. 1). WiFi Aps and LTE femtocells have different EIRP values. Therefore, the total number of the optimization variables is 850. We will compare the results from three different network planning design cases. The cases will be for High Definition (HD) video coverage, HD video coverage with low exposure, and Standard Definition (SD) video coverage. To test the algorithms ' performance we have selected cases that are quite demanding regarding low exposure limits and high coverage.

We compare MOBBO with NSGA-II and GDE3. The algorithms are executed 20 times. The best results

are compared. It must be pointed out that the control parameters selected for both NSGA-II and GDE3 algorithms are those that commonly perform well regardless of the characteristics of the problem to be solved. All algorithms are initialized with a population size of 200 and run for 1000 iterations. The control parameters chosen for GDE3 are according to [22, 50] $F = 0.5, CR = 0.1$. The authors of GDE3 in [22, 50] claim that these are considered to be good parameter choices. For MOBBO, we set the habitat modification probability, $P_{\text{mod}}$, to 1 and the maximum mutation rate, $m_{\max}$, equal to 0.001. The maximum immigration rate *I*, and the maximum emigration rate *E* are both set to one. For NSGA-II [27] we have set the crossover and mutation probabilities equal to 0.9 and 0.1, respectively. The crossover probability is chosen to be 0.9 in the original NSGA-II paper [27]. We must also point out that the mutation probability is selected to be *1/D* in [27] but the problems have a maximum of 30 dimensions. We have instead after a trial-and-error procedure selected the value 0.1 for NSGA-II for this problem. Therefore, the control parameters for both NSGA-II and GDE3 are considered to be good choices. All algorithms are compiled using the same compiler (Microsoft Visual C++ 2010) in a PC with Intel Core i5-2410M, at 2.30GHz with 4GB RAM running Windows 7.

### *4.1 Performance Indicators for Multi-Objective Algorithms*

In order to compare the Pareto fronts found by various different algorithms suitable performance indicators for multi-objective evolutionary will be used [51, 52]. A (unary) quality indicator is a function that assigns to each Pareto set approximation a real number. Therefore, a unary quality indicator *I* can be defined as a mapping from the set of all approximations sets $\Omega$ to the set of real numbers $I : \Omega \to \mathbf{R}$.

In the following results we will use the performance indicators [52]:

1) The Hypervolume difference to a reference set $I_{\bar{H}}$.The hypervolume indicator $I_H$ measures the hypervolume of the portion of objective space that is weakly dominated by an approximation set *A*. The hypervolume indicator $I_H$ is to be maximized. The $I_{\bar{H}}(A)$ for a given approximation set *A* is defined by

$$I_{\bar{H}}(A) = I_H(R) - I_H(A) \tag{20}$$

where *R* is a reference set obtained by the union of the non-dominated approximation sets found by all algorithms. Therefore, the reference set *R* is an approximation of the Pareto front.

2) The Unary epsilon indicator $I_{\varepsilon 1}$. This indicator is based on the binary epsilon-indicator. The binary epsilon-indicator $I_\varepsilon(A,B)$ gives the maximum $\varepsilon$ factor by which each point in $B$ can be multiplied such that the resulting approximation set is weakly dominated by *A*:

$$I_\varepsilon(A,B) = \inf_{\varepsilon \in R} \left\{ \forall z_2 \in B \;\; \exists z_1 \in A : z_1 \preceq_\varepsilon z_2 \right\} \tag{21}$$

where the $\varepsilon-$dominance relation $\preceq_\varepsilon$ is defined as:

$$z_1 \preceq_\varepsilon z_2 \Leftrightarrow \forall i \in 1..n : z_{i,1} \le \varepsilon z_{i,2} \tag{22}$$

The Unary epsilon indicator $I_{\varepsilon 1}(A)$ for a given approximation set *A* is defined by:

$$I_{\varepsilon 1}(A) = I_\varepsilon(A,R) \tag{23}$$

3) The R2 indicator is used to compare approximation sets on the basis of a set of utility functions. A utility function $u$ maps from the set $Z$ of objective space vectors to the set $\mathbf{R}$ of real numbers $u : Z \to \mathbf{R}$. The R2 indicator $I_{R2}$ given by [52]:

$$I_{R2}(A) = \frac{\sum_{\lambda \in \Lambda} u^*(\bar{\lambda}, A) - u^*(\bar{\lambda}, R)}{|\Lambda|} \tag{24}$$

where $u^*$ is the maximum value reached by the utility function $u$ with weight vector $\bar{\lambda}$ on an approximation set A, i.e. $u^*(\bar{\lambda}, A) = \max_{z \in A} u(z)$, $\Lambda$ is a set of weight vectors that contain weight combinations $\bar{\lambda}$ with $\forall i \in 1..n : \lambda_n \ge 0 \wedge \sum_{j=1}^{n} \lambda_j = 1$.

The utility function we choose is the augmented Tchebycheff function given by [52]:

$$u(z) = -\left( \max_{j \in 1..n} \lambda_j \left| z_j^* - z_j \right| + \rho \sum_{j \in 1..n} \left| z_j^* - z_j \right| \right) \tag{25}$$

Where $\rho$ is a sufficiently small positive number. For all the above-mentioned quality indicators the smaller values indicate better Pareto front approximations. More details about performance assessment of multi-objective stochastic algorithms can be found in [52]. It must be pointed out that along with the quality indicators we have compared the three algorithms regarding computational time.

*4.2 Best compromised solution*

In order to choose the best compromised solution from the Pareto Front a suitable decision maker has to used. The fuzzy set theory has been used as a decision maker in several applications in the literature like transportation planning, vendor selection, etc. [53, 54]. The satisfaction degree of each objective function is represented by a linear fuzzy membership function expressed as

$$\mu_k = \begin{cases} 1 \;\; if \;\; z_k \le z_k^{\min} \\ \dfrac{z_k^{\max} - z_k}{z_k^{\max} - z_k^{\min}} \;\; if \;\; z_k^{\min} < z_k < z_k^{\max} \\ 0 \;\; if \;\; z_k \ge z_k^{\max} \end{cases} \tag{26}$$

where $z_k$ the value of k-th objective function, $z_k^{\min}$, $z_k^{\max}$ are the minimum and maximum value of the k-th objective function respectively. The best compromised solution is found by using

$$s = \frac{1}{n_{obj}} \sum_{k=1}^{n_{obj}} \mu_k \tag{27}$$

where $n_{obj}$ is the number of objectives and s is the degree of satisfaction.

For each Pareto Front point, we calculate the value of s. The point with the maximum s value is the best compromised solution.

*4.3 Pareto fronts and performance indicators*

The first example is that of case 1, which assumes High Definition (HD) video coverage (receiver sensitivity set to -68dBm and -68.1dBm for WiFi and LTE respectively) for all points with coverage limit $C_{limit} = 99\%, E_{limit} = 0.25V/m$ . The sensitivies above correspond to 54Mbps throughput for WiFi and 40Mbps for LTE respectively. The exposure limit is low in order to test the algorithms' performance on demanding cases.

The 3D Pareto fronts for this case found by all algorithms are shown in Fig. 4. Each point of the Pareto front denotes a feasible network configuration. We notice that NSGA-II obtained Pareto fronts with a larger number of APs than GDE3 and MOBBO. The tradeoff for this case is the lower electric field values. The Pareto Fronts obtained by MOBBO and GDE3 are comparable. Both algorithms have obtained an almost equal number of non-dominated solutions 60 and 65 for MOBBO and GDE3 respectively.

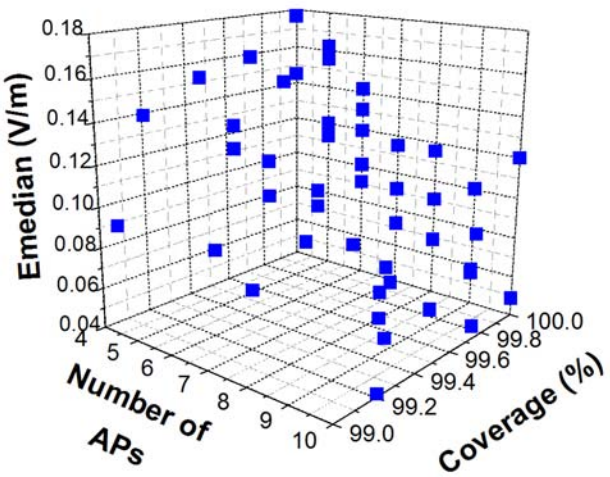


(a)

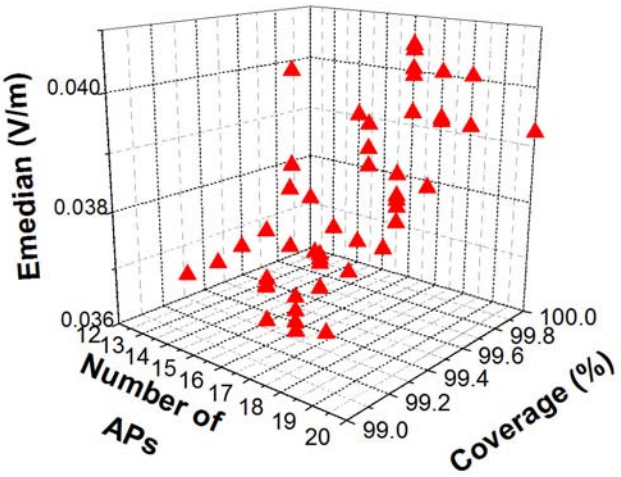


(b)

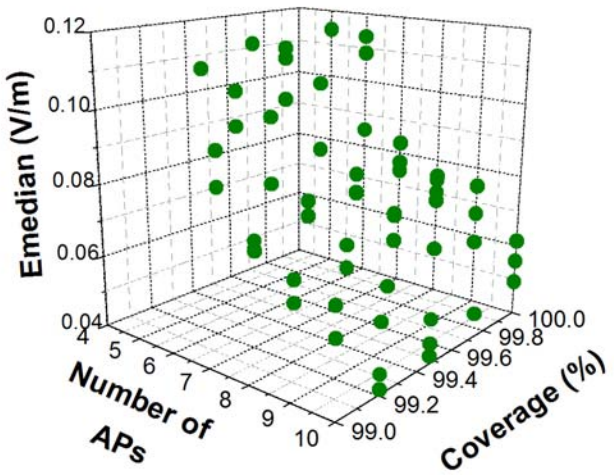


(c)

Fig. 4 Pareto fronts for case 1 found by (a) MOBBO, (b) NSGA-II and (c) GDE3.

The second case example assumes also HD video coverage for all points with coverage limit $C_{limit} = 99\%, E_{limit} = 0.04V/m$ . One may notice that the exposure is set to extremely low. Again, our objective is to force the algorithms to find solutions for complex cases.

Fig. 5 depicts the Pareto fronts found by all algorithms. It is obvious for this case that MOBBO outperforms NSGA-II and GDE3. One may notice that the range of APs for MOBBO is from 12 to 14. The other algorithms for the same exposure and coverage range have obtained solutions that range from 12 to

21 and from 17, which indicates that these solutions are dominated by those obtained by MOBBO. The number of Pareto front points is 21, 15, and 15 for MOBBO, NSGA-II and GDE3 respectively.

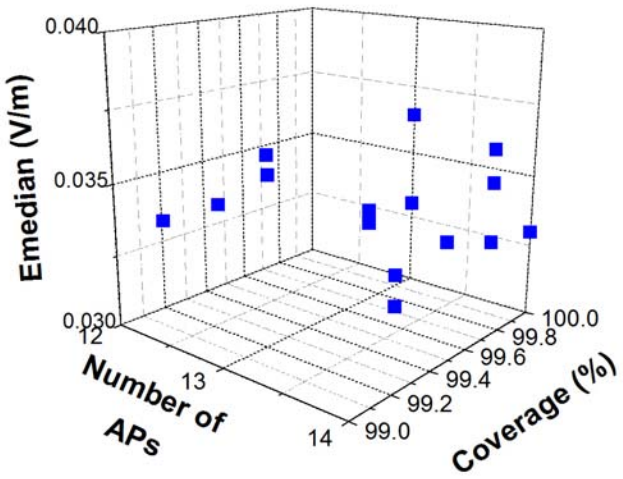


(a)

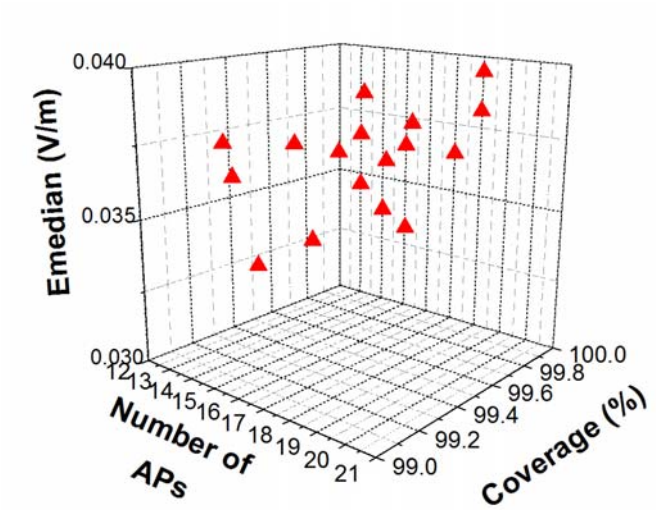


(b)

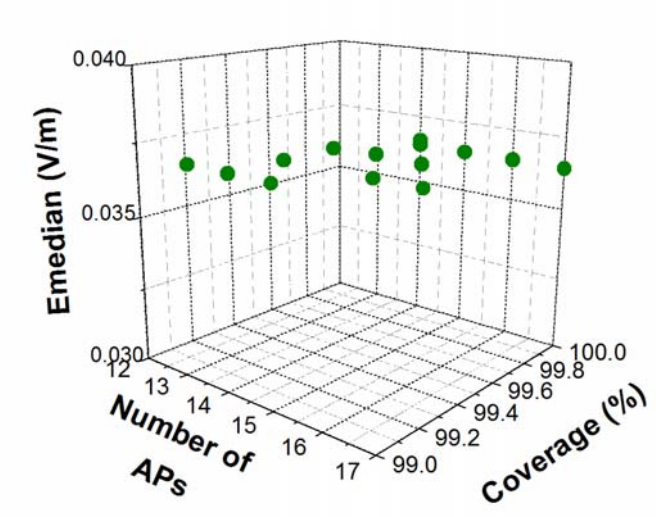


(c)

Fig. 5 Pareto fronts for case 2 found by (a) MOBBO, (b) NSGA-II and (c) GDE3.

The final example presents a network layout where 25Mpbs video (SD) is required for all points. The receiver sensitivity is set to -79dBm and -77.1dBm for WiFi and LTE respectively. The constraints for this case are $C_{limit} = 99\%, E_{limit} = 0.1V/m$ . For this case we assume that a LTE femtocell is always present with EIRP=10 dBm at a specific position. This is the heterogeneous case, consisting of both WiFi Aps and LTE femtocells. The Pareto fronts found are shown in Fig. 6. The APs range for MOBBO is from 3 to 7. The NSGA-II for the same exposure and coverage range obtained solutions that range from five to eight. GDE3 also obtained solutions with AP number that varies from three to eight.

Table 1. Performance indicators of the MOEAs. the Smallervalues are in bold ( $I_H$ =Hypervolume difference indicator , $I_{\varepsilon 1}$ = Unary epsilon indicator $I_{R2}$ = R2 indicator)

| **Case 1:HD video coverage** $C_{limit} = 99\%, E_{limit} = 0.25V/m$ | | | |
|---|---|---|---|
| Performance Indicator | MOBBO | GDE3 | NSGA-II |
| $I_{\bar{H}}$ | 0.064 | **0.047** | 0.474 |
| $I_{\varepsilon 1}$ | **0.084** | 0.090 | 0.500 |

| | | | |
|---|---|---|---|
| $I_{R2}$ | **0.006** | 0.007 | 0.117 |
| Average time (sec) | 1681.7 | 1785.4 | **1449.2** |
| **Case 2:HD video coverage with low exposure** $C_{limit} = 99\%, E_{limit} = 0.04V / m$ | | | |
| Performance Indicator | MOBBO | GDE3 | NSGA-II |
| $I_{\bar{H}}$ | **0.024** | 0.559 | 0.083 |
| $I_{\varepsilon 1}$ | **0.100** | 0.445 | 0.200 |
| $I_{R2}$ | **0.002** | 0.124 | 0.021 |
| Average time (sec) | **1228.1** | 1778.2 | 1410 |
| **Case 3:SD video coverage** $C_{limit} = 99\%, E_{limit} = 0.1V / m$ | | | |
| Performance Indicator | MOBBO | GDE3 | NSGA-II |
| $I_{\bar{H}}$ | **0.039** | 0.073 | 0.352 |
| $I_{\varepsilon 1}$ | **0.200** | **0.200** | 0.400 |
| $I_{R2}$ | **0.002** | 0.016 | 0.083 |
| Average time (sec) | 835.4 | 885.2 | **827.3** |

The quality of the Pareto fronts found is measured using the performance indicators in Table 1. The best values are the smaller ones. For case 1, the MOBBO and GDE3 values are close, while both outperform NSGA-II. In this case, NSGA-II requires slightly less computational time than GDE3 and MOBBO for the same number of objective functions evaluations. NSGA-II has found the smallest number of Pareto points than the other algorithms. For case 2, as it could be expected from the Pareto Fronts, MOBBO clearly outperforms the other algorithms. The MOBBO algorithm for this case requires slightly less computational

time than the other algorithms. In case 3, MOBBO outperforms the other algorithms in terms of performance indicators, while GDE3 outperforms NSGA-II. In terms of computational time, NSGA-II is slightly faster than the other algorithms. We notice that MOBBO in all three cases obtained the best results in terms of performance indicators. GDE3 has also performed well and its results are close to that of MOBBO. In terms of computational time NSGA-II is in general slighly faster than the other algorithms. This could be due to the lower computational complexity of NSGA-II compared with the other algorithms. It is also evident from the results that NSGA-II performs better for lower exposure limits.

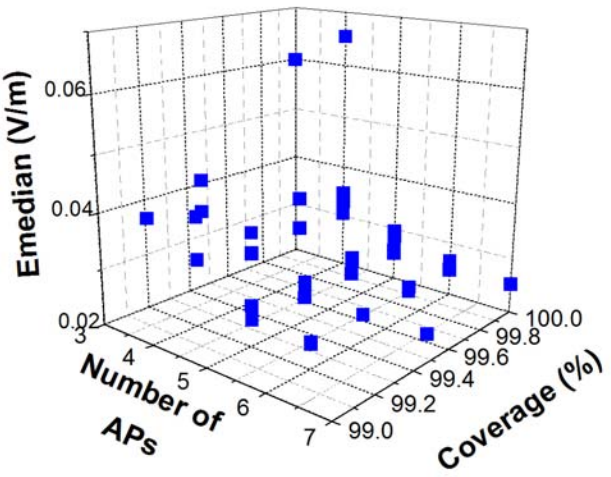


(a)

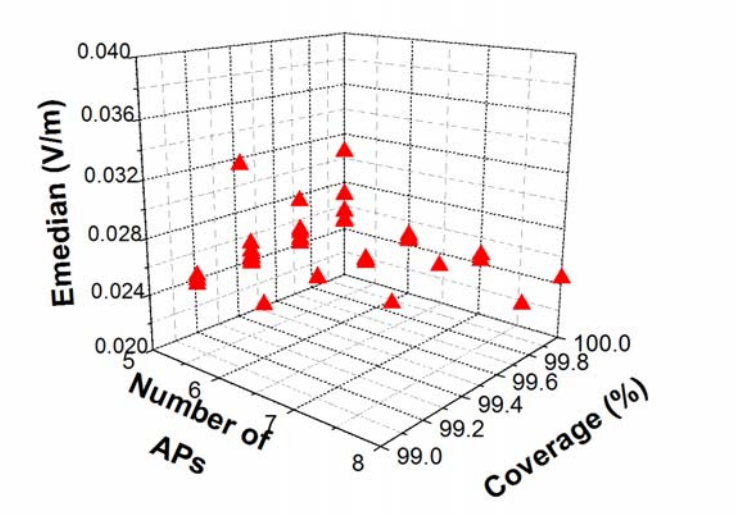


(b)

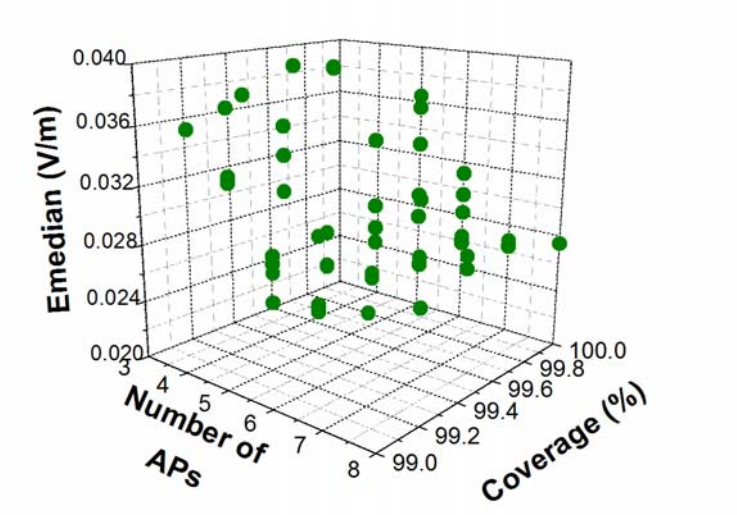


(c)

Fig. 6 Pareto fronts for case 3 found by (a) MOBBO, (b) NSGA-II and (c) GDE3.

### *4.4 Best Solutions: comparison of algorithms*

Table 2 reports the best compromised solutions found by all algorithms in the three cases. It must be pointed out that comparison between different MOEAs is performed using the performance indicators given in Table 1. These performance indicators compare the whole set of solutions that each algorithms

produces. In cases, where single solutions from the above algorithms are used like in this section one might not directly conclude which algorithm performs better. For example, if we obtain two solutions from two solution sets then these solutions could be non-dominated. In that case, it cannot be directly concluded that one algorithm is better than the other. We notice that for case 1 MOBBO obtained the solution with the lowest number of APs. The solution found by NSGA-II is that with the lowest electric-field value. One might notice that these solutions are non-dominated. For case 2 the AP number is larger than 10 in all algorithms. This is due to the low exposure limit of 0.04 V/m, set in order to oblige the algorithms to place several APs with low power levels, satisfying the coverage requirement. The MOBBO obtained result has fewer APs (13) and a lower field exposure (0.033 V/m). This solution dominates the solutions found by the other algorithms. The results for case 3 also differ. The number of APs is lower than that of the other cases. As could be expected, the lower smartphone (Wifi and LTE) receiver sensitivity results in fewer APs needed. We notice that the solution obtained by MOBBO is the one with the lowest number of APs. The solution obtained by NSGA-II is the one with the lowest exposure value. We notice that the E-field standard deviation values are lower for lower exposure limits. This implies that the E-field distribution is more homogeneous for these cases. We also notice that the solutions obtained by NSGA-II are the ones with the lower standard deviation values. The tradeoff for lower AP number (thus lower power consumption) is higher field exposure values and larger dispersion of E-field values. All three solutions are non-dominated.

The network layout and the E-field distribution for the best configurations obtained by MOBBO is shown in Figs 7a-7c. Again, case 2 (Fig 7b) is the one with the highest number of APs, while the least APs are present for case 1 (least strict exposure limit). In case 3 (Fig. 7c), the LTE femtocell (EIRP of 10 dBm) and wiFi Aps are indicated. It is evident that increasing the number of APs results to lower exposure values and more homogeneous E-field distribution.

Table 2. Best compromised solutions

| **Case 1:HD video coverage** |
|---|

| $C_{limit} = 99\%, E_{limit} = 0.25V / m$ | | | | |
|---|---|---|---|---|
| **Algorithm** | **Number of APs** | **Coverage (%)** | **Emedian (V/m)** | **Std. Dev.** |
| MOBBO | 5 | 100 | 0.113 | 0.142 |
| NSGA-II | 13 | 100 | 0.037 | 0.045 |
| GDE3 | 6 | 100 | 0.085 | 0.112 |
| **Case 2:HD video coverage with low exposure** $C_{limit} = 99\%, E_{limit} = 0.04V / m$ | | | | |
| **Algorithm** | **Number of APs** | **Coverage (%)** | **Emedian (V/m)** | **Std. Dev.** |
| MOBBO | 13 | 100 | 0.033 | 0.031 |
| NSGA-II | 15 | 100 | 0.036 | 0.030 |
| GDE3 | 14 | 100 | 0.033 | 0.031 |
| **Case 3:SD video coverage** $C_{limit} = 99\%, E_{limit} = 0.1V / m$ | | | | |
| **Algorithm** | **Number of APs** | **Coverage (%)** | **Emedian (V/m)** | **Std. Dev.** |
| MOBBO | 4 | 100 | 0.030 | 0.058 |
| NSGA-II | 6 | 100 | 0.024 | 0.043 |
| GDE3 | 5 | 100 | 0.027 | 0.101 |

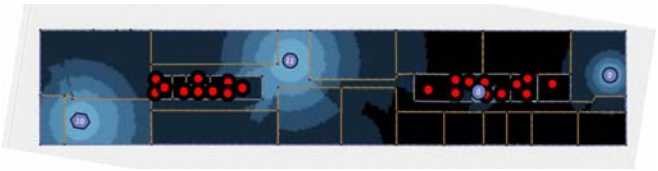

(a)

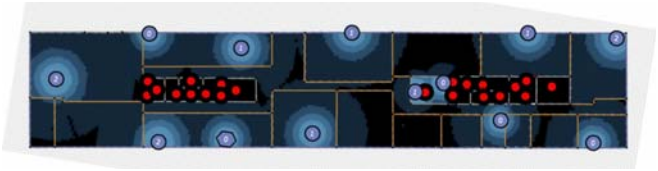

(b)

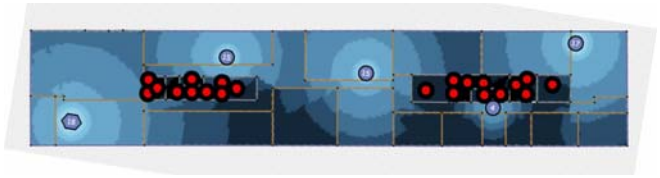

(c)

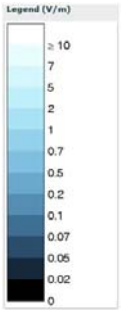


Fig 7. Network layout of best-compromised solutions found by MOBBO a) Case 1 b) Case 2 c) Case 3. (WiFi AP = dot, LTE femtocell = hexagon, EIRP is indicated within dot or hexagon).

## 5. Conclusion

The problem of heterogeneous (LTE and WiFi) network planning for optimal coverage with the lowest power consumption and the lowest exposure is addressed in this paper. An application for a realistic office environment is investigated leading to reductions of cost and exposure when multi-objective algorithms are applied. We proposed a multi-objective algorithm based on BBO and the concept of non-dominated ranking. MOBBO has been compared against NSGA-II and GDE3 for the network planning problem. MOBBO and GDE3 are quite efficient in producing the Pareto front for design cases. They produce better results than NGSA-II for the same population size and for the same number of generations. MOBBO produced better results than GDE3 for all design cases. This is also shown by the calculation of performance indicators suitable for multi-objective evolutionary algorithms.

The numerical results obtained by multi-objective algorithms allow the network engineer the possibility of selecting from a set of optimal solutions. All the above algorithms can be easily applied to different network planning problems. In our future work, we intend to examine different network configurations using different constraints. Additionally, possible modifications of the MOBBO algorithm will be

examined. These could include the modification of the migration models and new mutation operators.

## References

[1] J. Zhang, X. Jia, Z. Zheng, Y. Zhou, Minimizing cost of placement of multi-radio and multi-power-level access points with rate adaptation in indoor environment, IEEE Transactions on Wireless Communications, 10 (2011) 2186-2195.
[2] W. Li, Y. Cui, X. Cheng, M.A. Al-Rodhaan, A. Al-Dhelaan, Achieving proportional fairness via AP power control in multi-rate WLANs, IEEE Transactions on Wireless Communications, 10 (2011) 3784-3792.
[3] I. Sohn, S.H. Lee, J.G. Andrews, Belief propagation for distributed downlink beamforming in cooperative MIMO cellular networks, IEEE Transactions on Wireless Communications, 10 (2011) 4140-4149.
[4] D. Cao, S. Zhou, Z. Niu, Improving the energy efficiency of two-tier heterogeneous cellular networks through partial spectrum reuse, IEEE Transactions on Wireless Communications, 12 (2013) 4129-4141.
[5] D. Cao, S. Zhou, Z. Niu, Optimal combination of base station densities for energy-efficient two-tier heterogeneous cellular networks, IEEE Transactions on Wireless Communications, 12 (2013) 4350-4362.
[6] Z. Zhao, Z. Peng, S. Zheng, J. Shang, Cognitive radio spectrum allocation using evolutionary algorithms, IEEE Transactions on Wireless Communications, 8 (2009) 4421-4425.
[7] Z. Ji, B.H. Li, H.X. Wang, H.Y. Chen, T.K. Sarkar, Efficient ray-tracing methods for propagation prediction for indoor wireless communications, IEEE Antennas and Propagation Magazine, 43 (2001) 41-49.
[8] R.P. Torres, L. Valle, M. Domingo, S. Loredo, M.C. Diez, CINDOOR: An engineering tool for planning and design of wireless systems in enclosed spaces, IEEE Antennas and Propagation Magazine, 41 (1999) 11-21.
[9] G. Wölfle, R. Wahl, P. Wertz, P. Wildbolz, F. Landstorfer, Dominant path prediction model for indoor scenarios, German Microwave Conference, (2005).
[10] S. Phaiboon, An empirically based path loss model for indoor wireless channels in laboratory building, IEEE Region 10 Annual International Conference, Proceedings/TENCON, 2 (2002) 1020-1023.
[11] J.M. Keenan, A.J. Motley, Radio coverage in buildings, British Telecom technology journal, 8 (1990) 19-24.
[12] D. Plets, W. Joseph, K. Vanhecke, E. Tanghe, L. Martens, Coverage prediction and optimization algorithms for indoor envi-ronments, EURASIP Journal On Wireless Communications and Networking, Special Issue On Radio Propagation, Channel Mod-eling, and Wireless, Channel Simulation Tools For Heterogeneous Networking Evaluation, 1 (2012).
[13] M. Deruyck, E. Tanghe, W. Joseph, L. Martens, Modelling and optimization of power consumption in wireless access networks, Computer Communications, 34 (2011) 2036-2046.
[14] D. Plets, W. Joseph, E.D. Poorter, L. Martens, I. Moerman, Concept and framework of a self-regulating symbiotic network, EURASIP Journal On Wireless Communications and Networking, 2012 (2012).
[15] W. Joseph, L. Verloock, F. Goeminne, G. Vermeeren, L. Martens, Assessment of RF exposures from emerging wireless communication technologies in different environments, Health Physics, 102 (2012) 161-172.
[16] IEEE, IEEE standard for safety levels with respect to human exposure to radio frequency electromagnetic fields, 3 kHz to 300 GHz, in: Std C95.1, 1999.
[17] A. Ahlbom, U. Bergqvist, J.H. Bernhardt, J.P. Cesarini, L.A. Court, M. Grandolfo, M. Hietanen, A.F. McKinlay, M.H. Repacholi, D.H. Sliney, J.A.J. Stolwijk, M.L. Swicord, L.D. Szabo, M. Taki, T.S. Tenforde, H.P. Jammet, R. Matthes, Guidelines for limiting exposure to time-varying electric, magnetic, and electromagnetic fields (up to 300 GHz), Health Physics, 74 (1998) 494-521.
[18] M. Deruyck, W. Vereecken, W. Joseph, B. Lannoo, M. Pickavet, L. Martens, Reducing the power consumption in wire-less access networks: Overview and recommendations, Progress In Electromagnetics Research, 132 (2012) 255-274.
[19] J. Kennedy, R. Eberhart, Particle swarm optimization, in: IEEE International Conference on Neural Networks, Piscataway, NJ, 1995, pp. 1942-1948.
[20] R. Storn, K. Price, Differential evolution - A simple and efficient heuristic for global optimization over continuous spaces, Journal of Global Optimization, 11 (1997) 341-359.
[21] S. Kukkonen, J. Lampinen, GDE3: the third evolution step of generalized differential evolution, in: Proceedings of the 2005 IEEE Congress on Evolutionary Computation, (CEC 2005). , 2005, pp. 443-450 Vol.441.
[22] S. Kukkonen, J. Lampinen, Performance assessment of Generalized Differential Evolution 3 (GDE3) with a given set of problems, in: Proceedings of the IEEE Congress on Evolutionary Computation, 2007. CEC 2007. , 2007, pp. 3593-3600.
[23] K.C. Tan, CEC 2007 Conference Report, IEEE Computational Intelligence Magazine, 3 (2008) 72-73.
[24] S.K. Goudos, J.N. Sahalos, Pareto optimal microwave filter design using multiobjective differential evolution, IEEE Transactions on Antennas and Propagation, 58 (2010) 132-144.
[25] S.K. Goudos, K. Siakavara, E.E. Vafiadis, J.N. Sahalos, Pareto optimal yagi-uda antenna design using multi-objective differential evolution, Progress in Electromagnetics Research, 105 (2010) 231-251.
[26] S.K. Goudos, K.A. Gotsis, K. Siakavara, E.E. Vafiadis, J.N. Sahalos, A multi-objective approach to subarrayed linear antenna arrays design based on memetic differential evolution, IEEE Transactions on Antennas and Propagation, 61 (2013) 3042-3052.
[27] K. Deb, A. Pratap, S. Agarwal, T. Meyarivan, A fast and elitist multiobjective genetic algorithm: NSGA-II, IEEE Transactions on Evolutionary Computation, 6 (2002) 182-197.
[28] J.O. Yang, Q.R. Yuan, F. Yang, H.J. Zhou, Z.P. Nie, Z.Q. Zhao, Synthesis of Conformal Phased Array With Improved NSGA-II Algorithm, IEEE Transactions on Antennas and Propagation 57 (2009) 4006-4009.
[29] W. Yao, S. Chen, S. Tan, L. Hanzo, Minimum bit error rate multiuser transmission designs using particle swarm optimisation, IEEE Transactions on Wireless Communications, 8 (2009) 5012-5017.
[30] D. Simon, Biogeography-Based Optimization, IEEE Transactions on Evolutionary Computation, 12 (2008) 702-713.
[31] M.A.C. Silva, L. dos S Coelho, R.Z. Freire, Biogeography-based Optimization approach based on Predator-Prey concepts applied to path planning of 3-DOF robot manipulator, in: 2010 IEEE Conference on Emerging Technologies and Factory Automation (ETFA), 2010, pp. 1-8.
[32] A. Rathi, A. Agarwal, A. Sharma, P. Jain, A new hybrid technique for solution of economic load dispatch problems based on Biogeography Based Optimization, in: TENCON 2011 - 2011 IEEE Region 10 Conference, 2011, pp. 19-24.
[33] P. Kankanala, S.C. Srivastava, A.K. Srivastava, N.N. Schulz, Optimal Control of Voltage and Power in a Multi-Zonal MVDC Shipboard Power System, IEEE Transactions on Power Systems, PP 1-9.

[34] S. Ashrafinia, U. Pareek, M. Naeem, D. Lee, Source and Relay Power Selection Using Biogeography-Based Optimization for Cognitive Radio Systems, in: 2011 IEEE Vehicular Technology Conference (VTC Fall), 2011, pp. 1-5.
[35] K.K. Mandal, B. Bhattacharya, B. Tudu, N. Chakraborty, A novel population-based optimization algorithm for optimal distribution capacitor planning, in: 2011 International Conference on Energy, Automation, and Signal (ICEAS), 2011, pp. 1-6.
[36] I. Boussaïd, A. Chatterjee, P. Siarry, M. Ahmed-Nacer, Hybridizing biogeography-based optimization with differential evolution for optimal power allocation in wireless sensor networks, IEEE Transactions on Vehicular Technology, 60 (2011) 2347-2353.
[37] K. Jamuna, K.S. Swarup, Power system observability Using Biogeography Based Optimization, in: International Conference on Sustainable Energy and Intelligent Systems (SEISCON 2011), 2011, pp. 384-389.
[38] A. Bhattacharya, P.K. Chattopadhyay, Biogeography-Based Optimization for Different Economic Load Dispatch Problems, IEEE Transactions on Power Systems, 25 (2010) 1064-1077.
[39] S.K. Goudos, K.B. Baltzis, K. Siakavara, T. Samaras, E. Vafiadis, J.N. Sahalos, Reducing the number of elements in linear arrays using biogeography-based optimization, in, Prague, 2012, pp. 1615-1618.
[40] K. Jamuna, K.S. Swarup, Multi-objective biogeography based optimization for optimal PMU placement, Appl. Soft Comput. J., 12 (2012) 1503-1510.
[41] X. Li, M. Yin, Multiobjective binary biogeography based optimization for feature selection using gene expression data, IEEE Transactions on Nanobioscience, 12 (2013) 343-353.
[42] H. Mo, Z. Xu, Q. Tang, Constrained multi-objective biogeography optimization algorithm for robot path planning, in, 2013, pp. 323-329.
[43] H.A. Nguyen, H. Guo, K.S. Low, Real-time estimation of sensor node's position using particle swarm optimization with log-barrier constraint, IEEE Trans. Instrum. Meas., 60 (2011) 3619-3628.
[44] F. Babich, A. Crismani, Cooperative coding schemes: Design and performance evaluation, IEEE Transactions on Wireless Communications, 11 (2012) 222-235.
[45] ITU-R recommendation P.1546, Method For Point-to-area Predictions For Terrestrial Services In the Frequency Range 30MHz to 3000 MHz, (2003-2005).
[46] D. Plets, W. Joseph, K. Vanhecke, L. Martens, Exposure optimization in indoor wireless networks by heuristic network planning, Progress In Electromagnetics Research, 139 (2013) 445-478.
[47] R.T. Marler, J.S. Arora, Survey of multi-objective optimization methods for engineering, Structural and Multidisciplinary Optimization, 26 (2004) 369-395.
[48] K. Deb, L. Thiele, M. Laumanns, E. Zitzler, Scalable Test Problems for Evolutionary Multiobjective Optimization, in: Evolutionary Multiobjective Optimization, 2005, pp. 105-145.
[49] S. Kukkonen, K. Deb, A fast and effective method for pruning of non-dominated solutions in many-objective problems, Lecture Notes in Computer Science, 4193 (2006) 553-562.
[50] S. Kukkonen, J. Lampinen, An Empirical Study of Control Parameters for The Third Version of Generalized Differential Evolution (GDE3), in: Proceedings of the IEEE Congress on Evolutionary Computation, 2006. CEC 2006., 2006, pp. 2002-2009.
[51] E. Zitzler, L. Thiele, M. Laumanns, C.M. Fonseca, V.G. Da Fonseca, Performance assessment of multiobjective optimizers: An analysis and review, IEEE Transactions on Evolutionary Computation, 7 (2003) 117-132.
[52] J. Knowles, L. Thiele, E. Zitzler, A tutorial on the performance assessment of stochastic multiobjective optimizers, TIK Report, 214 (2006).
[53] J.K. Lain, Joint transmit/receive antenna selection for MIMO systems: A real-valued genetic approach, IEEE Communications Letters, 15 (2011) 58-60.
[54] W. Cheng, H. Shi, X. Yin, D. Li, An Elitism strategy based Genetic Algorithm for streaming pattern discovery in wireless sensor networks, IEEE Communications Letters, 15 (2011) 419-421.